PS/DL/LEAR Note 81-1
$\bar{p}p$ LEAR Note 90
6.2.1981

ANTINEUTRON PRODUCTION WITH AN INTERNAL TARGET IN THE LEAR MAGNET

K. Kilian, D. Möhl

1. INTRODUCTION

Useful beams of antineutrons [1] can be produced by $\bar{p}p$ interactions at LEAR. In this context, internal target operation combined with phase-space cooling has several advantages [2]: small target volume, good energy resolution, low background, no multiple interactions and last but not least a high antiproton economy. As explained in Ref. 2), the high efficiency results because losses due to multiple Coulomb scattering on the target are counteracted by cooling. Ideally then, unwanted $\bar{p}$ losses (i.e. losses by effects other than by strong interactions) occur only by Coulomb scattering into angles larger than the acceptance angle Θ_{ap} of the storage ring. The resulting efficiency for strong interaction $E = E(\Theta_{ap},p)$, which is a function of Θ_{ap} and of the particle momentum p was worked out in Ref. 2) and is reproduced here in Fig. 1 which also includes a comparison to the efficiency of an external transmission target E.

2. THE IMPORTANCE OF A LOW BETA

At high momenta Coulomb interactions can be neglected and we have $E \approx 1$. At low momenta where Coulomb scattering becomes strong $E \propto \Theta_{ap}^2$ and a large Θ_{ap} is desirable to ensure a reasonable efficiency E.

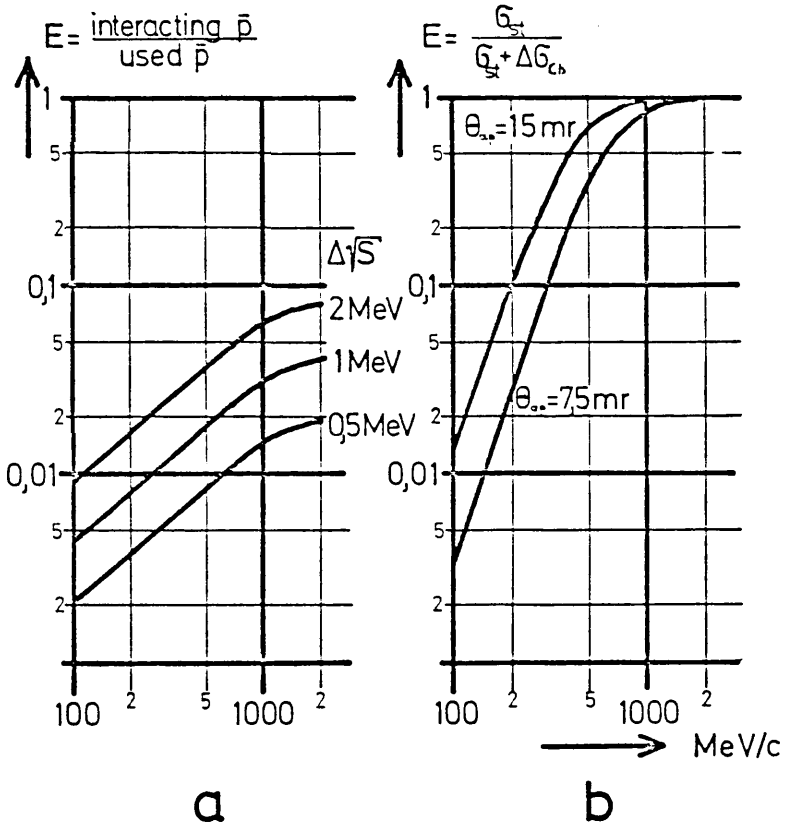

Fig. 1 Target efficiencies: a) on an external hydrogen transmission target with a thickness chosen to give a certain resolution; b) on an internal hydrogen gas target with perfect phase-space cooling.

It is for this reason that Ref. 2) suggested to place the target into a "low beta" point of the ring where the beam is strongly focussed, so that large divergencies Θ_{ap} are permitted.

In fact the acceptance angle Θ at any point s in the ring can be expressed in terms of the acceptable phase-space area A and the function $\beta(s)$ which characterizes the focussing properties of the ring (see Ref. 3)).

$$\Theta = \sqrt{A/(\pi \cdot \beta(s))} \qquad (1)$$

Equation (1) holds for horizontal and vertical quantities separately. In order to work out Coulomb losses, an average (see Appendix) has to be taken

$$\theta_{ap} \approx \sqrt{\frac{2}{1/\theta_h^2+1/\theta_v^2}} \approx \sqrt{\theta_h \theta_v} \qquad (2)$$

Equation (1) underlines the importance of low β values at the target and of a large acceptance $A = \pi a_c^2/\beta_c$ (i.e. of a large aperture a_c and a small value β_c of the focussing function at the aperture limit).

3. TARGET LOCATIONS IN LEAR

An obvious low β point in LEAR is the center of a long straight section (see Figs. 2 and 3, taken from Ref. 7)) where θ_{ap} is about 4.5 mr under normal conditions or $\approx$ 15 mr when four additional quadrupoles are used to create a "low beta insertion" (Ref. 4)). A disadvantage of this target position is, however, that secondaries ($\bar{n}$) produced around zero degrees have to pass about 9 m through the beam pipe before they leave the machine through a bending magnet. Therefore, an external beam with only $\approx$ 75 μsterad of useful solid angle can be obtained (a cone with an aperture of $\pm$ 3 mr in the vertical and $\pm$ 8 mr in the horizontal plane corresponding to an aperture limitation of $\pm$ 27 $\times$ $\pm$ 70 mm^2).

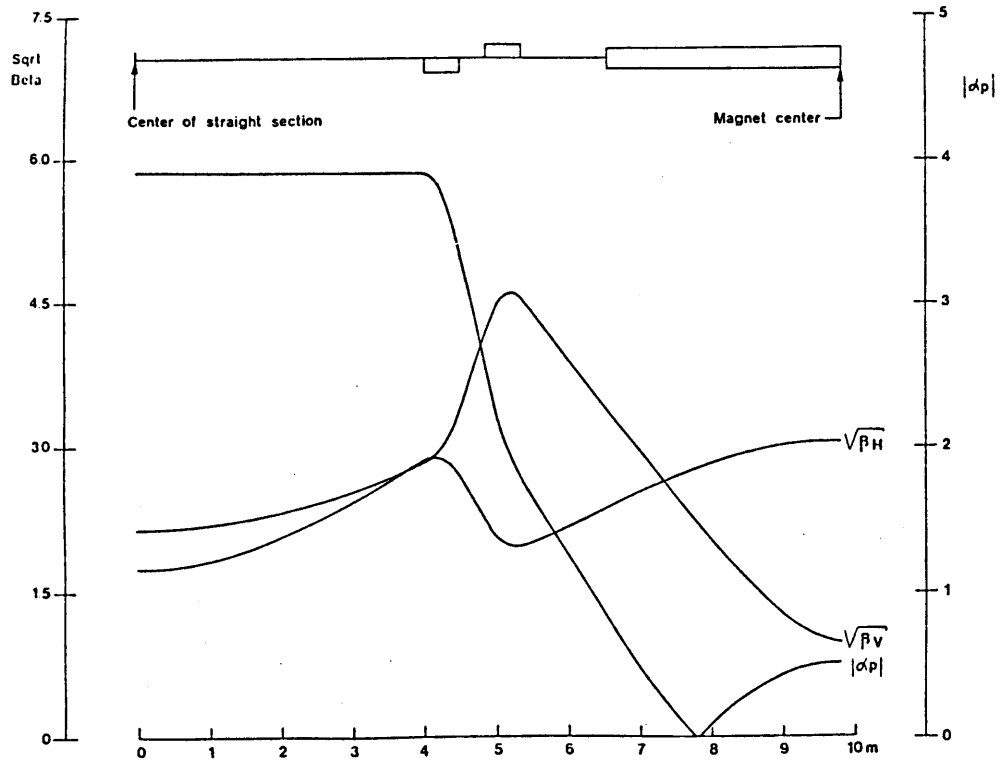

Fig. 2 Plot of twiss parameters for Lear doublet lattice QH = 2.3, QV = 2.7

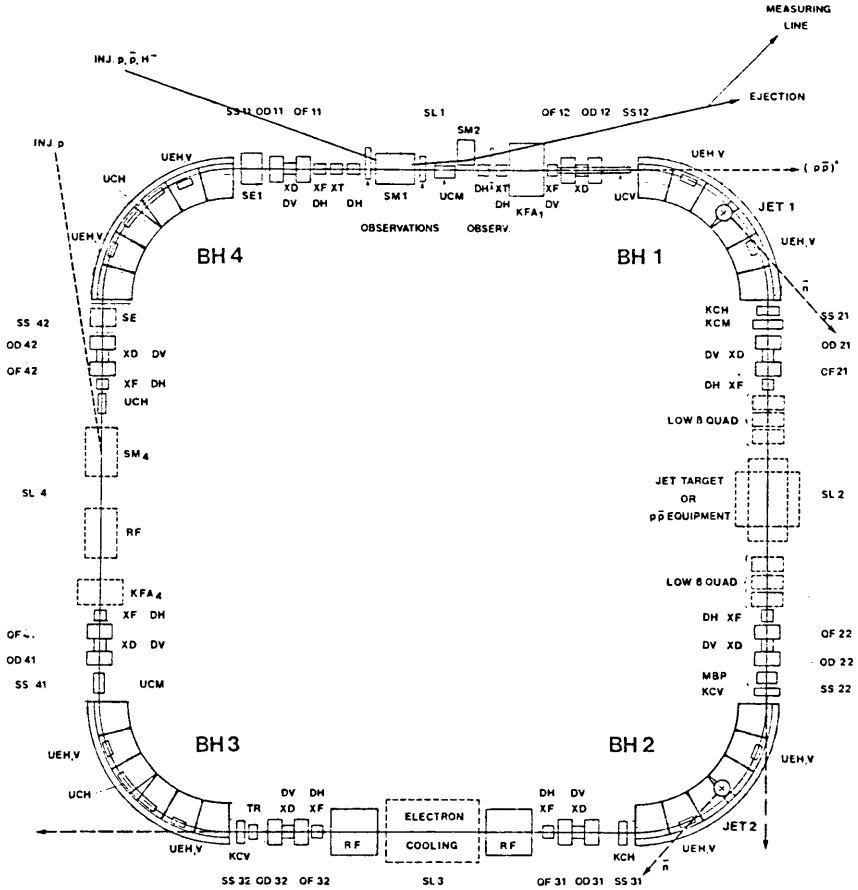

Fig.3
LEAR General Lay-out
(TENTATIVE, ELEMENTS OUT OF SCALE)
SCALE 1 50

A particularity of the LEAR lattice is that relatively low β values also occur in the center of the 90^{o} magnets (Fig. 2). This observation led us to the proposal to place the antineutron production target into the magnet center. It was therefore decided in 1979 to leave a wedge-shaped vertical gap of 15^{o} opening angle (24 cm width above the orbit, see Figs. 4 and 5, taken from Ref. 7)) in the centers of all 4 bending magnets, and to reserve two of these locations for the later introduction of a jet target.

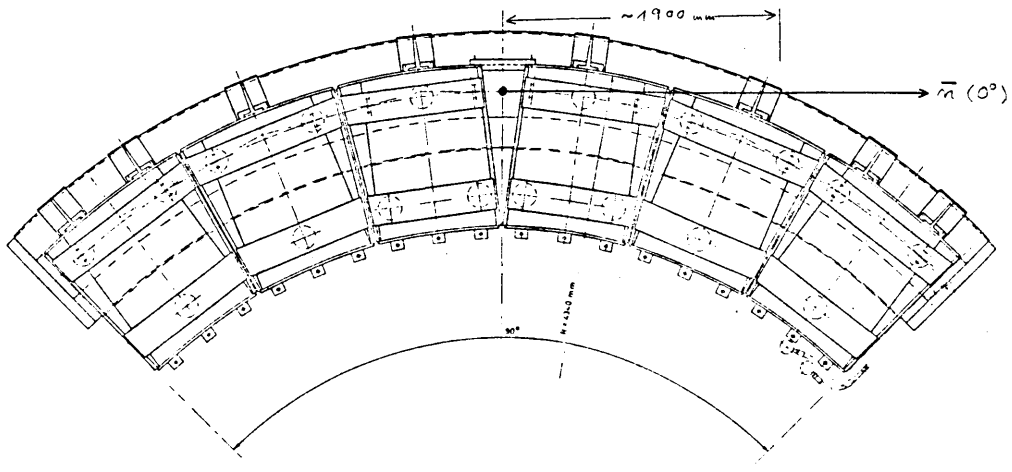

Fig. 4 : LEAR bending magnet

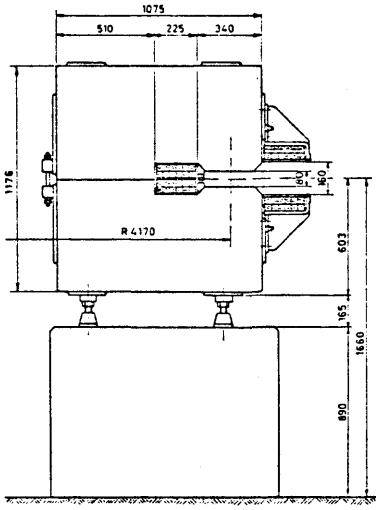

Fig. 5 : LEAR bending magnet

The acceptance angle in this position is $\theta_{ap} \gtrsim 6$ mr and the produced $\bar{n}$ leave the machine less than 2 meters downstream of the jet target. A flux with a solid angle of $\Delta\Omega \gtrsim 1500$ μsterad ($\psi_v \gtrsim \pm 15$ mr, $\psi_h \gtrsim \pm 35$ mr) can thus be used assuming the same aperture limitation as taken above. This assumption will be made for the purpose of comparing different target locations, although for the target in the magnet one could hope to make a much larger horizontal opening available.

We now define the useful $\bar{n}$ rate $R_{\bar{n}}$ in terms of the number ($r_{\bar{p}}$) of anti-protons available per second (say, $r_{\bar{p}} \approx 10^6$ $\bar{p}$/s) as:

$$R_{\bar{n}} = \frac{r_{\bar{n}}}{r_{\bar{p}}} = B_{\bar{n}} \cdot F(\Delta\Omega) \cdot E(\theta_{ap}, p) \qquad (3)$$

$B_{\bar{n}} \approx 6\times10^{-2}$ is here the branching ratio for the charge exchange (CEX) reaction $\bar{p}p \to \bar{n}n$. $F(\Delta\Omega) = \left[\int_{\Delta\Omega} d\sigma/d\Omega\ (CEX)\right]/\sigma_{tot}(CEX)$ characterizes the angular distribution of the $\bar{n}$ flux. $F(4\pi) \equiv 1$ and for small solid angles $\Delta\Omega$ one has $F(\Delta\Omega) \propto \Delta\Omega$ (for values of $d\sigma/d\Omega$, see Refs. 1) and 5)). The useful $\bar{n}$ rate is therefore

$$R_{\bar{n}} \propto \Delta\Omega \cdot E(\theta_{ap}, p)$$

and we may regard $\Delta\Omega \cdot E$ as a figure of merit for the target location. This quantity is worked out in Table 1 for different target situations. One concludes that the location in the magnets compares favourably even with respect to the low beta insertion in the straight section. In fact, the larger solid angle available in the magnet overcompensates the lower efficiency due to stronger Coulomb losses. The gain is 3 at low and as large as 20 at high momentum where $E(\theta_{ap}, p) \to 1$ for both locations. By further reducing the beta in the magnet the efficiency at low momentum can probably be further pushed.

TABLE 1

Target / Location	Θ_{ap} in mr	$\Delta\Omega$ in μsterad	figure for merit $\Delta\Omega \cdot E$ for 100 MeV/c	figure for merit $\Delta\Omega \cdot E$ for 2000 MeV/c
center of straight section, normal	4.5	0.075	$9.5 \cdot 10^{-5}$	$7.5 \cdot 10^{-2}$
center of straight section, low β	15	0.075	$1.05 \cdot 10^{-3}$	$7.5 \cdot 10^{-2}$
dipole center, normal machine configuration	6	1.5	$3.4 \cdot 10^{-3}$	1.5

An additional advantage may be of interest: the target in the magnet leaves straight section 2 free for other experimental apparatus.

The above comparison has been made for $\bar{n}$ beams produced around zero degrees. These beams have the advantage of small energy spread and high phase-space density. Sacrificing this advantage one may obtain much higher $\bar{n}$ fluxes appropriate for certain experiments by accepting large solid angles [6]. This is possible, e.g. by placing a large $\bar{n}$ interaction target close to the first low β quadrupole in the straight section. However, in this case the central cone of the $\bar{n}$ flux is not accessible.

4. SPECIAL PROBLEMS OF A TARGET IN THE MAGNET

The operation of an internal gas target requires the installation of large pumping capacity: up to 0.5 bar liter per second right at the source at pressures below 0.1 mbar are required [7]. For this purpose,

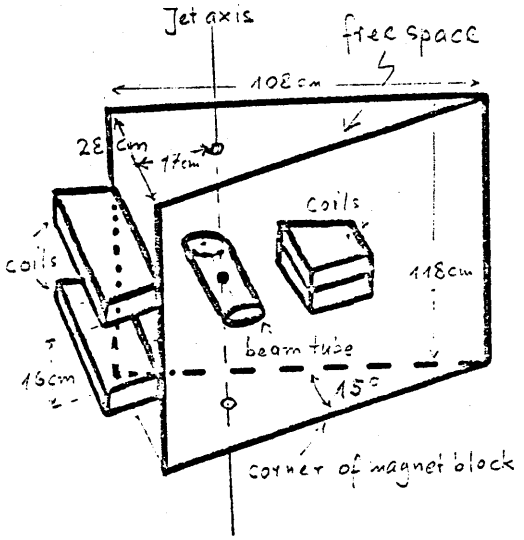

Fig. 6 Sketch of the free space around the jet position. Solid lines indicate limits of magnet blocks, coils and beam tube.

one needs large apertures for the gas transport to the vacuum and UHV pumps. The small distance from the vertical gas jet to the corners of the magnet blocks ($\lesssim$ 17 cm), the aperture of the C magnet which gives access to the beam tube between the coils, the opening of the wedge-shaped free space ($\approx$ 24 cm along the beam) and the relatively small fraction of this surface occupied by the coils of the magnet (see Fig. 6), leaves access, so that the necessary pumping speed can hopefully be installed. (A 10×10 cm aperture limits the vacuum conductance to $\sim$ 3500 ℓ/s for hydrogen at room temperature.) Moreover, one could think of installing UHV pumping systems (cryo, sublimation, getter) in the inner portion of the wedge aperture (Fig. 6) very close to the gas jet. Clearly, these questions have to be studied in more detail before a final design of the jet can be presented. However, we are hopeful that solutions are possible despite of the very stringent boundary conditions given by the presence of the magnet blocks and the needs of an ultra-high vacuum in the beam chamber.

5. ALTERNATIVE SOLUTIONS

Finally, we want to draw attention to a possibility to install an orbit bump in the low β section in straight section 2 (Fig. 7). This could allow to extract $\bar{n}$ flux around 0^{o} production angle sidewards from the straight section under a large solid angle and with the large strong interaction efficiency of the ss position. It is evident that such an installation is most attractive for low-energy operation. Just there the requirements for the dipoles which have to produce the strong orbit bump are less stringent. However, the problem of beam optics in the ring may be very critical.

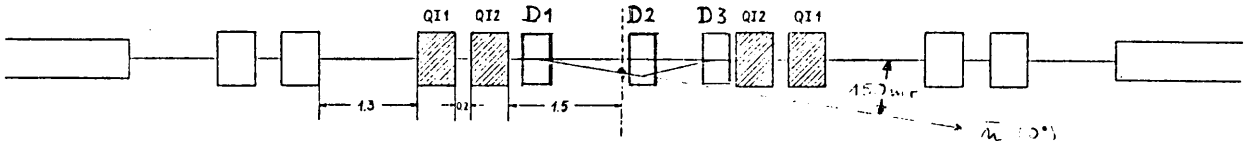

Fig. 7 Solution with orbit bump in a low β section with 3 additional dipoles D1-3.

REFERENCES

1) C. Voci, Antineutrons at LEAR, in Proc. of the Joint CERN-KFK Workshop on Physics with cooled low energy antiprotons, Karlsruhe, March 19-21 (1979), (KFK report 2836, editor H. Poth).

H. Poth, $\bar{n}$ beams from external targets, CERN $\bar{p}$p LEAR Note 15 and 52 (1979).

2) K. Kilian, D. Möhl, Gas jet target in LEAR, CERN $\bar{p}$p LEAR Note 44 (1979).

3) E. Courant, H. Snyder, Ann. Phys. (N.Y.) 3, 1 (1958);

M. Sands, SLAC-121 (1970).

4) J. Jäger, A low beta insertion for LEAR, CERN/PS/DL/LEAR Note 80-1 and CERN $\bar{p}$p LEAR Note 89.

5) B.S. Chaudhary et al., in Symposium on antinucleon-nucleon interactions, Prag 1974, p. 90-101, CERN Yellow Report 74-18 (editor L. Montanet).

6) H. Poth, Ref. 1) above and private communications.

7) Design study of a facility for experiments with low energy antiprotons (LEAR), CERN-PS-DL 80-7 (editor G. Plass).

Distribution

Distribution of abstract:

PS Scientific Staff (PS/1 list)

/ed

A P P E N D I X

AVERAGE ACCEPTANCE FOR COULOMB SCATTERING

Let the differential cross-section for the deflection of a particle in the Coulomb field of an atom be given by Rutherford's formula

$$\frac{d\sigma}{d\Omega} = \left(\frac{2Zr_e m_e c}{p\beta}\right)^2 \frac{1}{\Theta^4} \qquad \text{(A1)}$$

p, βc	momentum and velocity of the particel (charge e)
Z	charge number of the atom
r_e	$= 2.8 \times 10^{-13}$ cm
$m_e c$	$= 0.511$ MeV/c
Θ	deflection angle (see sketch)

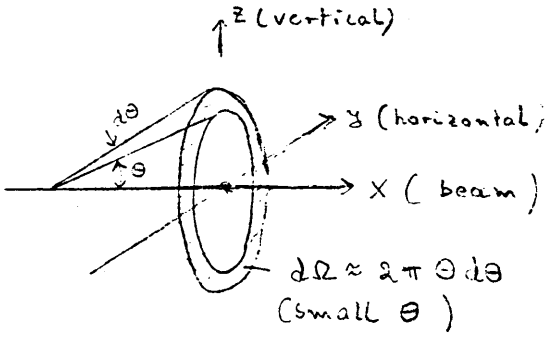

Traversing a length dx in a material containing L atoms per cm^3 the probability for a single scattering event with an angle larger than Θ_o is therefore

$$P(\Theta > \Theta_o) = \int_{\Theta_o}^{\hat{\Theta}} (L\, dx \frac{d\sigma}{d\Omega}) \frac{2\pi\Theta d\Theta}{\Theta^4} = C\, (\frac{1}{\Theta_o^2} - \frac{1}{\hat{\Theta}^2})$$

where

$$C = \pi L\, dx \left\{ \frac{2Z r_e m_e c}{p\beta} \right\}^2$$

(and for a hydrogen target of say 10^{-9} g/cm^2 "thickness"

$$L\, dx = \frac{10^{-9}}{m_p} \approx 6 \times 10^{14} \text{ atoms/cm}^2).$$

In (A2) $\hat{\theta} \approx (0.15 \text{ radian})/(A^{1/3}\, \beta\gamma)$ is the maximum angle permissible due to the finite size of the nucleus (see e.g. Jackson, Classical electrodynamics, Sect. 13.7). In the energy range of LEAR $\hat{\theta} \geq 70$ mr for hydrogen and the aperture angle is $\theta_o \lesssim 20$ mr. Hence, the second term in (A2) can be neglected and we have

$$P(\theta > \theta_o) \approx \frac{C}{\theta_o^2} . \qquad \text{(A3)}$$

To work out particle losses in a storage ring we have to average (A3) over the boundary $\theta_a(y,z)$ given by the acceptance (vacuum chamber) of the machine. For a rectangular chamber this was done by S. van der Meer (internal memo CERN/PS/AA/SvdM 78-1). We repeat the calculation here for an elliptical aperture limit which is more appropriate for LEAR.

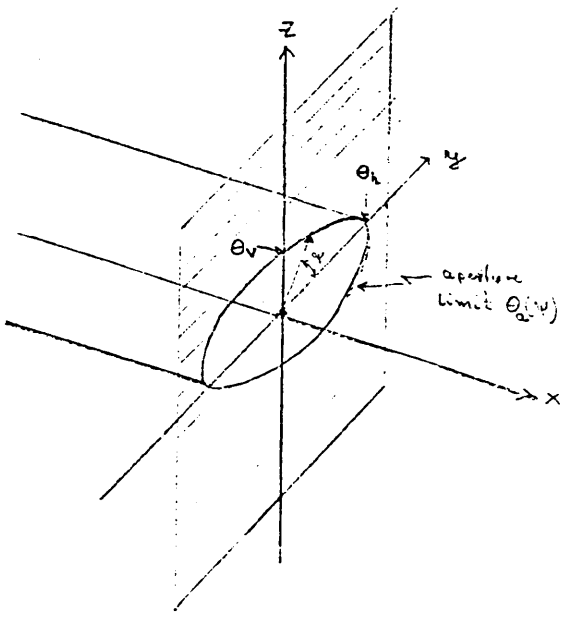

Fig. 9

Introducing the polar angle Ψ around the ideal orbit we may represent the aperture ellipse by

$$\frac{1}{\Theta_o^2(\Psi)} = \frac{\cos^2 \Psi}{\Theta_h^2} + \frac{\sin^2 \Psi}{\Theta_v^2} \; .$$

Observing that all scattering directions Ψ are equally probable we find the average of (A3) taking

$$< P\left(\Theta > \Theta_o(\Psi)\right) > = \frac{C}{2\pi} \int_o^{2\pi} \frac{d\Psi}{\Theta_o^2(\Psi)} = \frac{C}{2}\left(\frac{1}{\Theta_h^2} + \frac{1}{\Theta_v^2}\right) ,$$

i.e. we can work out single scattering losses from (A3) inserting the "average" angle

$$\Theta_{ap}^2 = \frac{2}{1/\Theta_h^2 + 1/\Theta_v^2} \; .$$

The corresponding expression for a rectangular chamber worked out by S. van der Meer is

$$\Theta_{ap}^2 = \pi \Theta_h \Theta_v \Big/ \left[1 + \frac{\Theta_h}{\Theta_v} \operatorname{atan} \frac{\Theta_h}{\Theta_v} + \frac{\Theta_v}{\Theta_h} \operatorname{atan} \frac{\Theta_v}{\Theta_h} \right] \; .$$

In both cases we obtain the loss rate for a thin beam in the center of the aperture. For a thick or an off-axis beam one has to apply an additional correction.

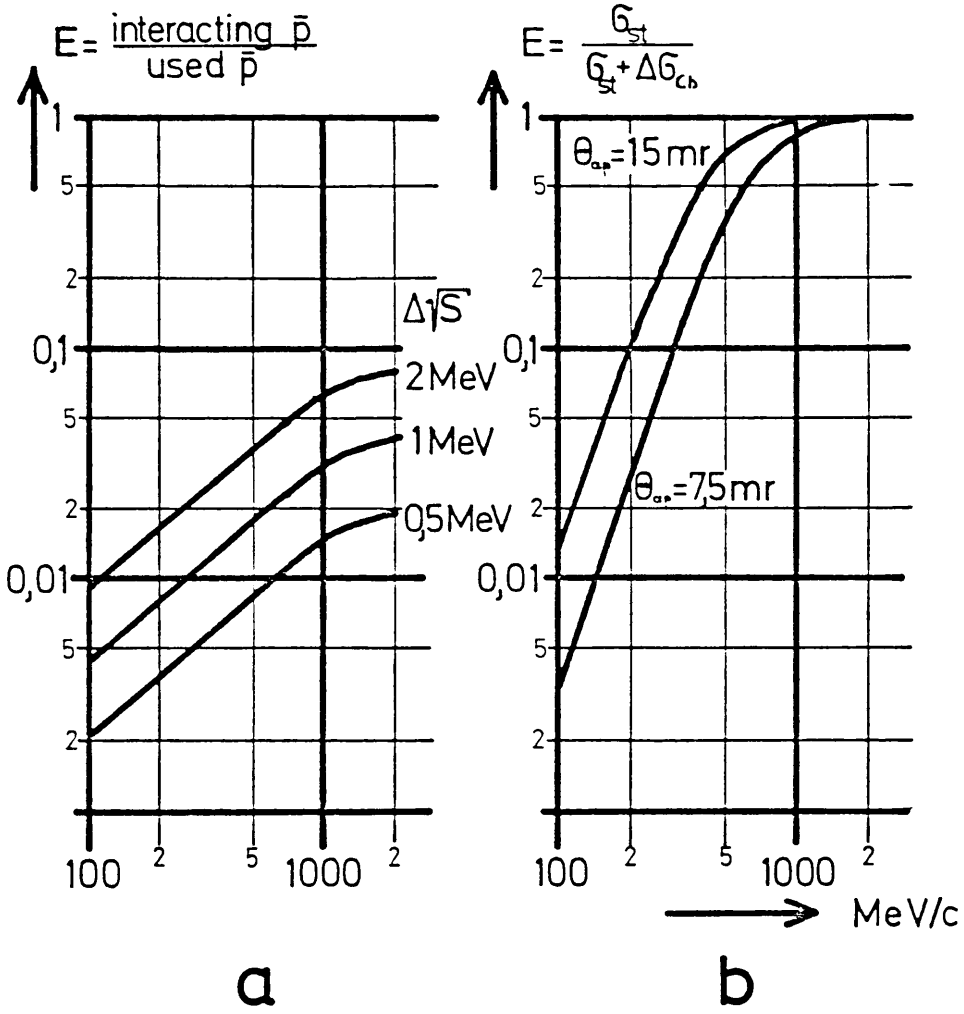

Fig. 1 Target efficiencies: a) on an external hydrogen transmission target with a thickness chosen to give a certain resolution; b) on an internal hydrogen gas target with perfect phase-space cooling.

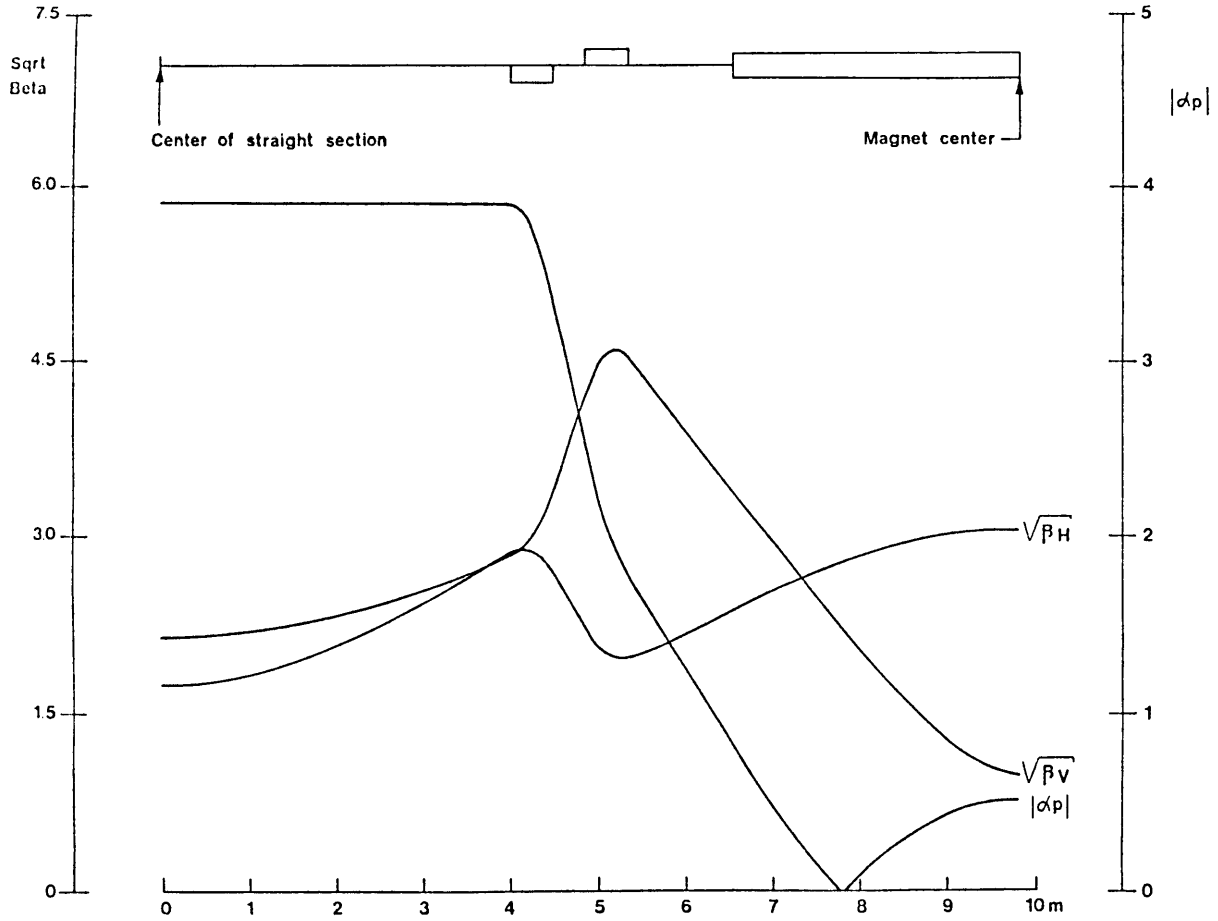

Fig. 2 Plot of twiss parameters for Lear doublet lattice QH = 2.3, QV = 2.7

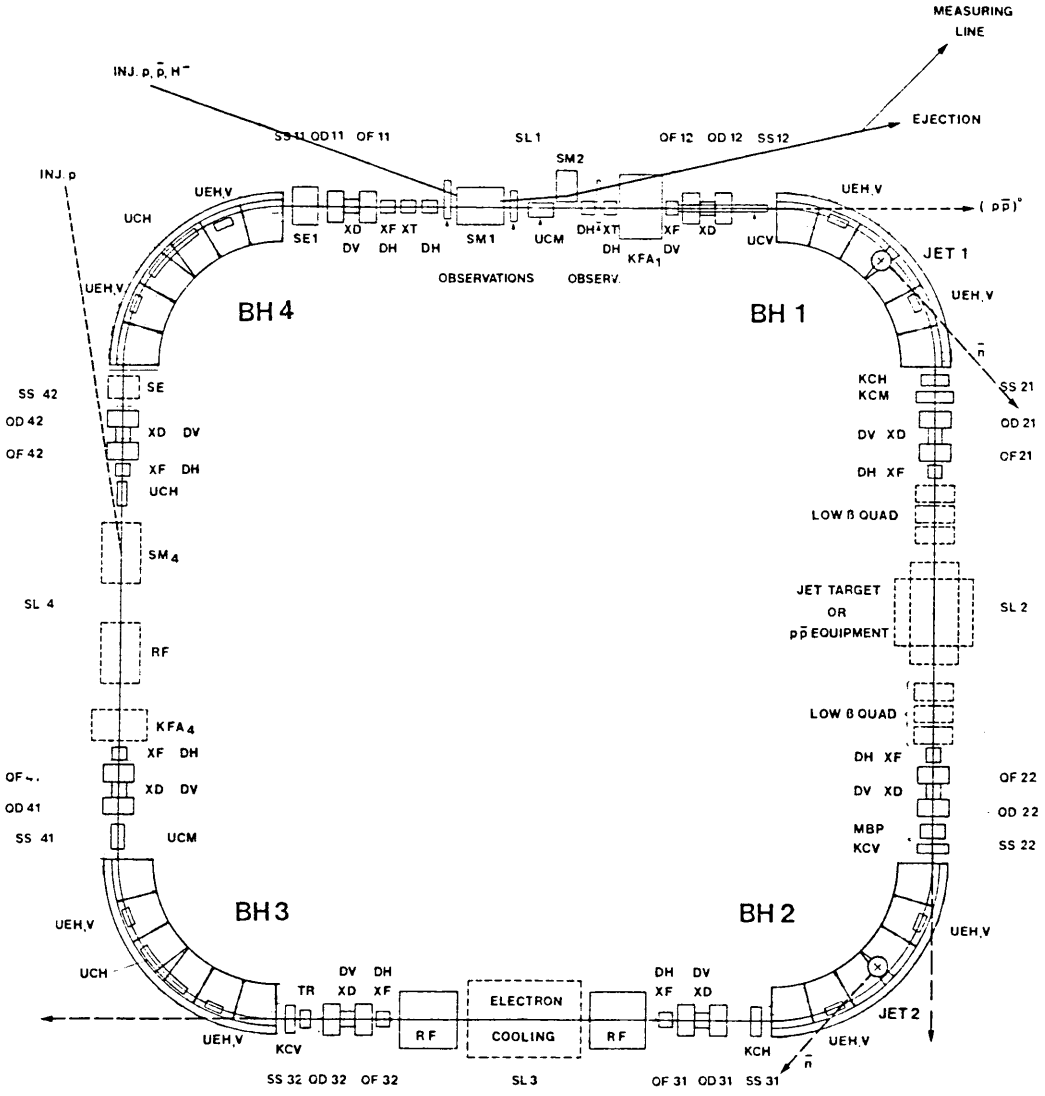

Fig.3

LEAR General Lay-out

(TENTATIVE, ELEMENTS OUT OF SCALE)

SCALE 1:50

SM

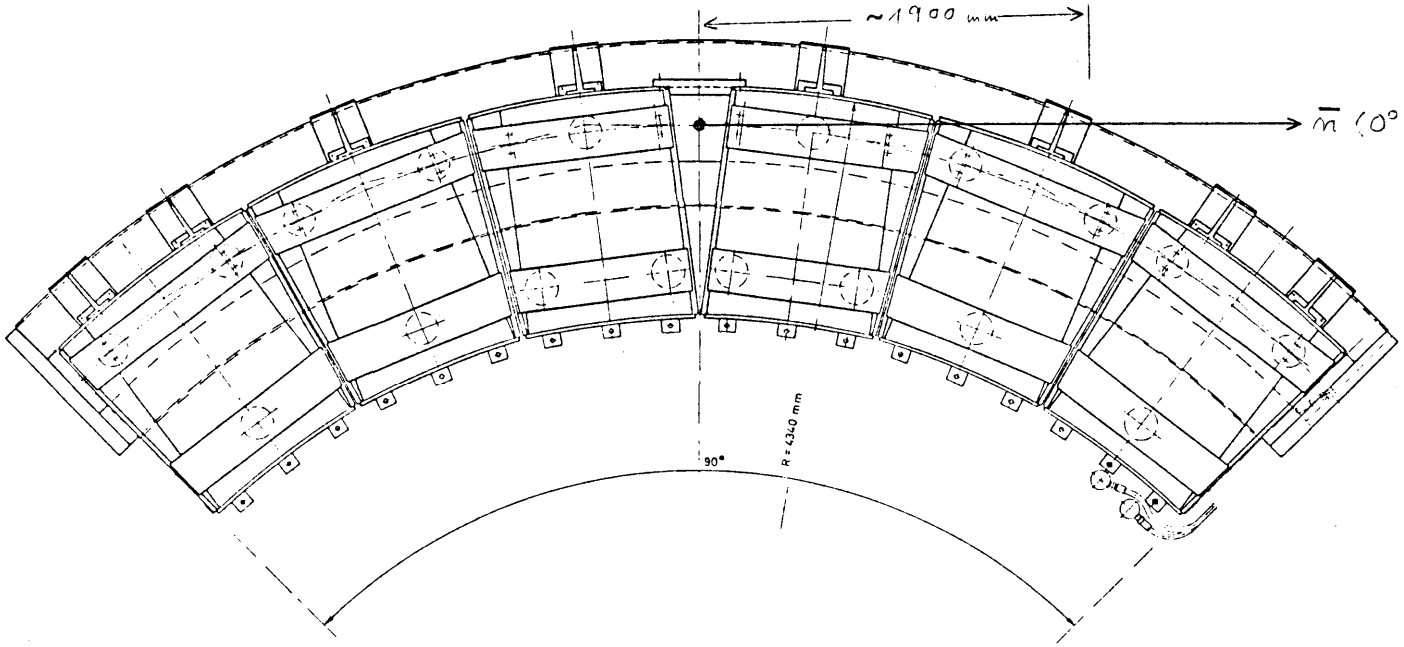

Fig. 4 : LEAR bending magnet

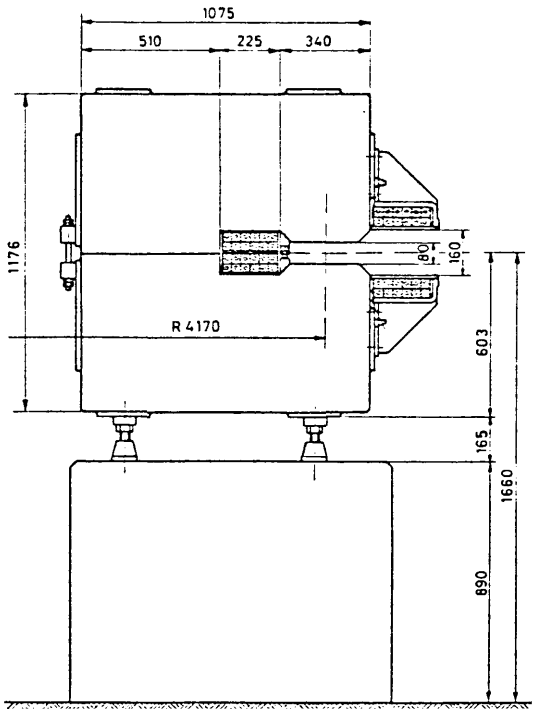

Fig. 5 : LEAR bending magnet

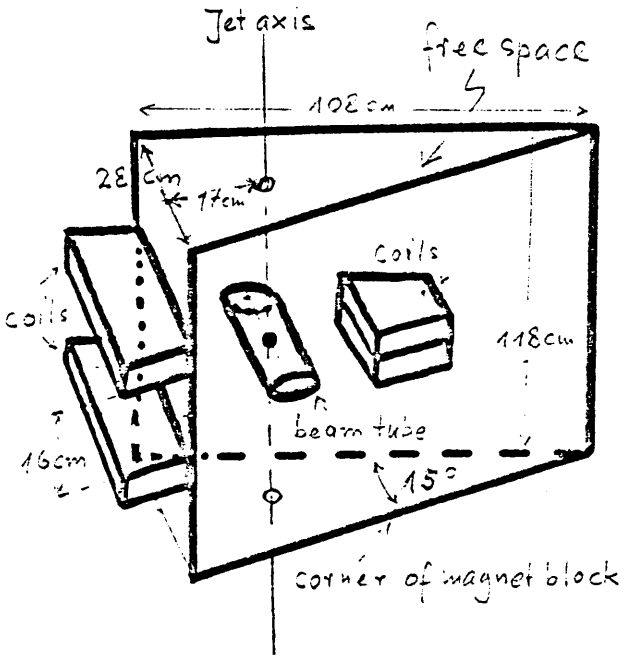

Fig. 6 Sketch of the free space around the jet position. Solid lines indicate limites of magnet blocks, coils and beam tube.

LEAR with low β and 4 additional quadrupoles